Supplementary Fig. 1 | Comparison between this study's ATAC-seq data and published accessibility data. **a**, Representative region showing the genome coverage of Ricci, Lu, Ji et al.'s ATAC-seq, Dong et al.'s ATAC-seq, Oka, Zicola, Weber et al.'s DNase-seq and Rodgers-Melnick et al.'s MNase-seq. In the MNase-seq tracks, the differential nuclease sensitivity (DNS) was calculated according to Rodgers-Melnick et al.'s methods. **b**, heatmap showing the reads or DNS signal enrichments around leaf and inflorescence ACR summits (the ACRs identified in this manuscript). 2 kb upstream to 2 kb downstream of ACR summits were plotted. **c**, Venn diagram showing the overlap among ACRs identified in this study versus the DNase hypersensitive sites identified by Oka, Zicola, Weber et al.

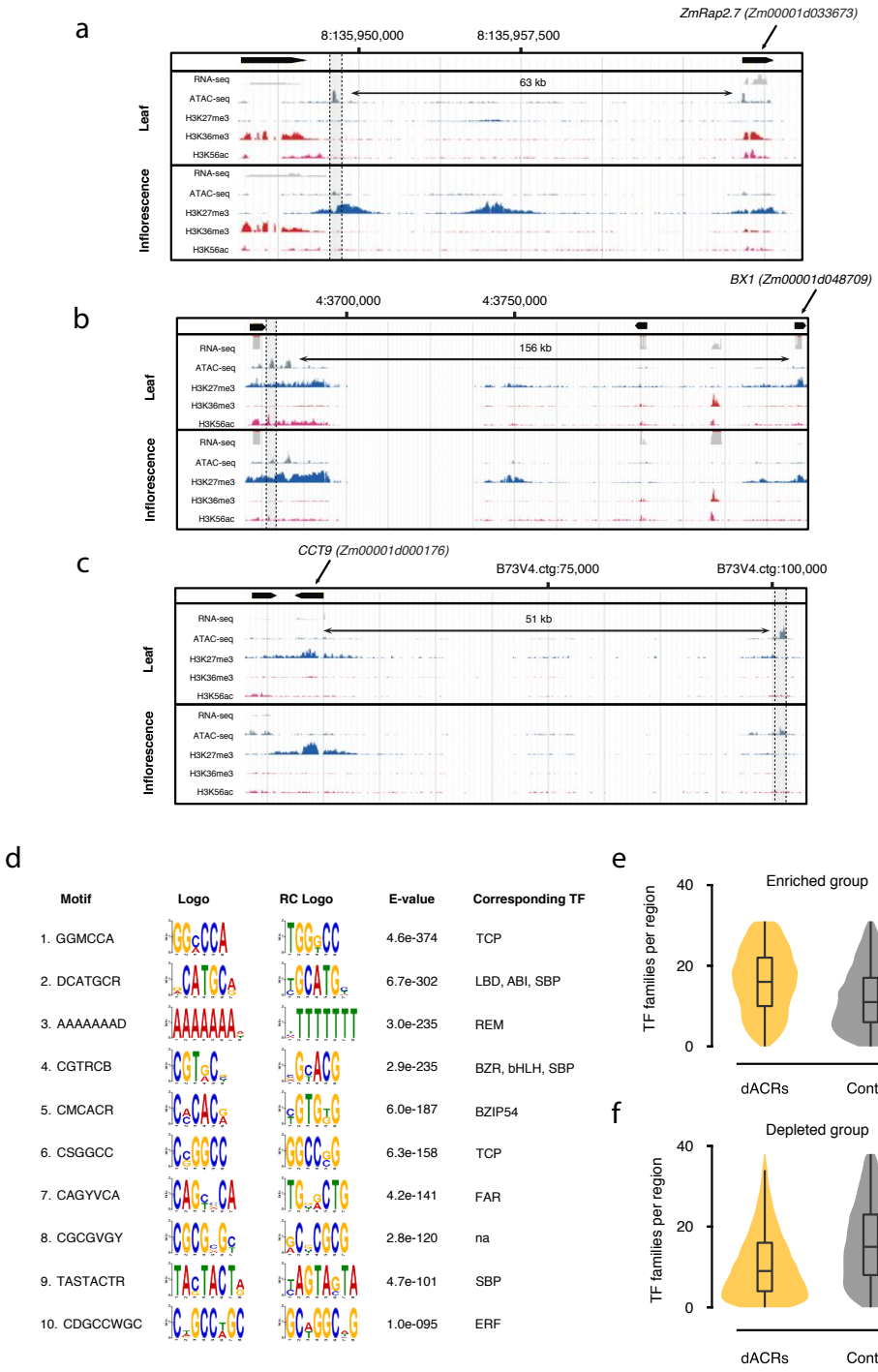

Supplementary Fig. 2 | Chromatin at genetically mapped CREs and TF binding site sequence enrichment in dACRs. a-c, ATAC-seq, ChIP-seq, and RNA-seq signal at agronomic maize genes and their genetically mapped hypothesized CREs (shaded); (a) *ZmRap2.7*, (b) *BX1*, (c) *ZmCCT9*. ATAC-seq and ChIP-seq experiments in a-c were performed in duplicate and yielded the same results both times. **d,** Motifs enriched within dACRs and corresponding TFs or TF families predicted to bind the motifs. **e-f,** count of TF families corresponding to *Arabidopsis*-derived motifs that are (e) enriched in dACRs and (f) depleted in dACRs. Shown in e and f are the results from 10,433 dACRs. Box plots in e and f comprise medians and quartiles.

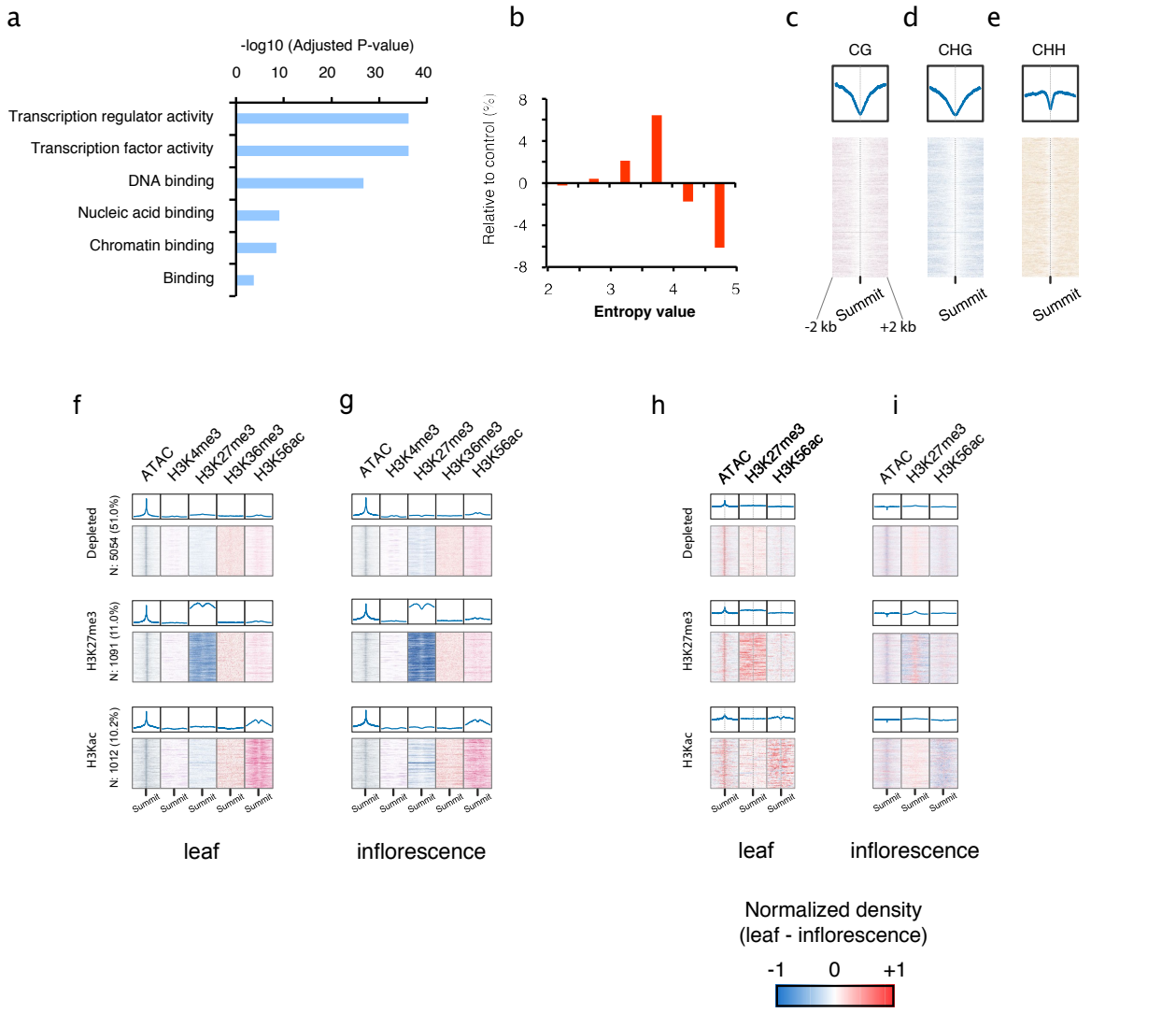

Supplementary Fig. 3 | Characteristics of genes flanking dACRs, DNA methylation depletion within dACRs, and histone modifications at differential dACRs. a, Enriched GO terms among genes that flank all dACRs. **b,** Gene expression entropy values of genes flanking all dACRs, relative to genes flanking negative intergenic controls. Control values were subtracted from experimental values. **c-e,** Cytosine methylation of dACRs, aligned by summits. Shown are the three methylation sequence contexts. **f,** ATAC-seq and ChIP-seq signal from leaf at all dACRs identified in leaf, split by the previously described chromatin groups. **g**, ATAC-seq and ChIP-seq signal from inflorescence, plotted at the same loci and sorted in the same order as in g. **h**, ATAC-seq and ChIP-seq signal at leaf-specific dACRs with the inflorescence signal subtracted from the leaf signal. Red indicates higher levels in leaf than in inflorescence. **i**, The reciprocal of h: ATAC-seq and ChIP-seq signal at inflorescence-specific dACRs with the inflorescence signal subtracted from the leaf signal. Red indicates higher levels in leaf than in inflorescence. ATAC-seq and ChIP-seq experiments shown in this figure were performed in duplicate and yielded the same results both times.

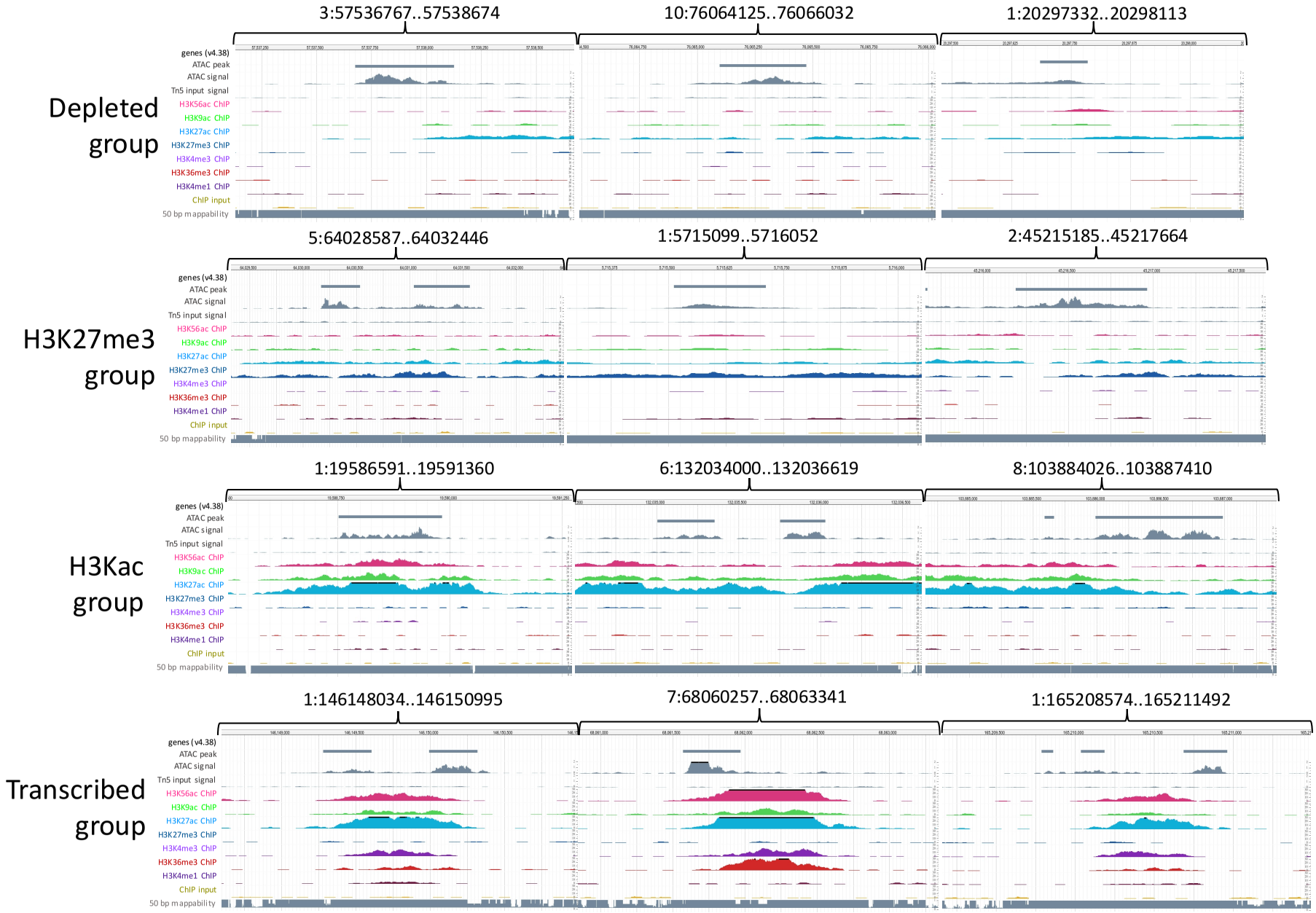
Depleted group
3:57536767..57538674
10:76064125..76066032
1:20297332..20298113
H3K27me3 group
5:64028587..64032446
1:5715099..5716052
2:45215185..45217664
H3Kac group
1:19586591..19591360
6:132034000..132036619
8:103884026..103887410
Transcribed group
1:146148034..146150995
7:68060257..68063341
1:165208574..165211492
genes (v4.38)
ATAC peak
ATAC signal
Tn5 input signal
H3K56ac ChIP
H3K9ac ChIP
H3K27ac ChIP
H3K27me3 ChIP
H3K4me3 ChIP
H3K36me3 ChIP
H3K4me1 ChIP
ChIP input
50 bp mappability

Supplementary Fig. 4 | Randomly selected loci of the dACR chromatin groups. For each of the four dACR groups described in fig. 2b-g, three loci were randomly selected. All y-axes are set to the same scales for ChIP-seq data. The strings above brackets indicate the coordinates in the B73 v4 reference genome. ATAC-seq and ChIP-seq experiments were performed in duplicate and yielded the same results both times.

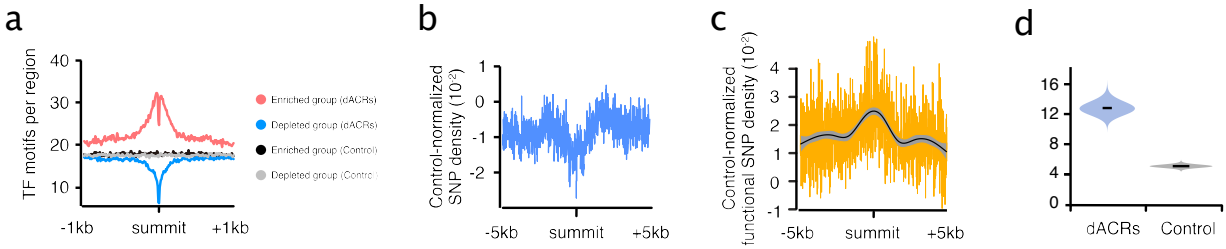

Supplementary Fig. 5 | The same analyses as in fig. 1h-k, but with the transcribed group dACRs omitted. **a,** Distribution of known TF binding motifs from Arabidopsis at dACR summits. **b,** Number of total SNPs among maize inbred lines or **c,** phenotype-associated SNPs per 100 bp bins flanking dACR summits. The negative control distribution was subtracted from the dACR distribution. **d,** Probability that a *cis*-eQTL's highest-significance SNP overlaps a dACR. Y-axis shows posterior probability. The center values correspond to the medians of the distributions. All figures use the same set of negative control regions (i.e. uniquely mapping, intergenic, non-accessible regions). Used for all figures were 10,130 negative control regions and 7,157 non-transcribed-group dACRs.

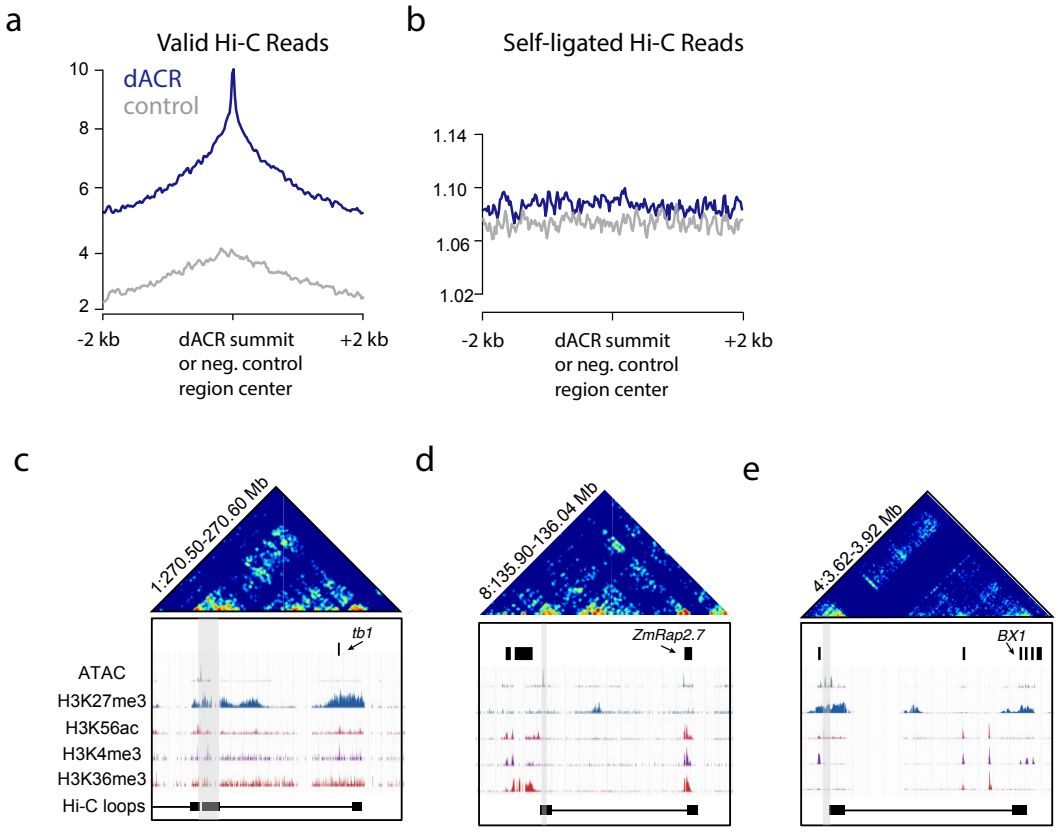

Supplementary Fig. 6 | Self-ligated Hi-C reads at dACRs and Hi-C loops identified between genes and their genetically mapped hypothesized CREs. a, Reads from valid Hi-C contact pairs (as determined by the Hi-C Pro pipeline) plotted at all dACRs (excluding the transcribed group) and plotted at all intergenic negative control regions. **b**, Reads from the self-ligated contact pairs plotted against the same regions. **c-e,** Hi-C detects interactions between the agronomic genes (c) *tb1*, (d) *ZmRap2.7*, (e) *BX1* and their genetically mapped controlling regions (shaded gray). Called Hi-C loops are shown in the bottom track. Heat maps display contacts at 500 bp resolution. The Hi-C loop passes over the *tb1* gene by a small margin, but H3K27me3 HiChIP loops directly overlap the gene (Fig. 4). The Hi-C experiment was analyzed as a single biological replicate.

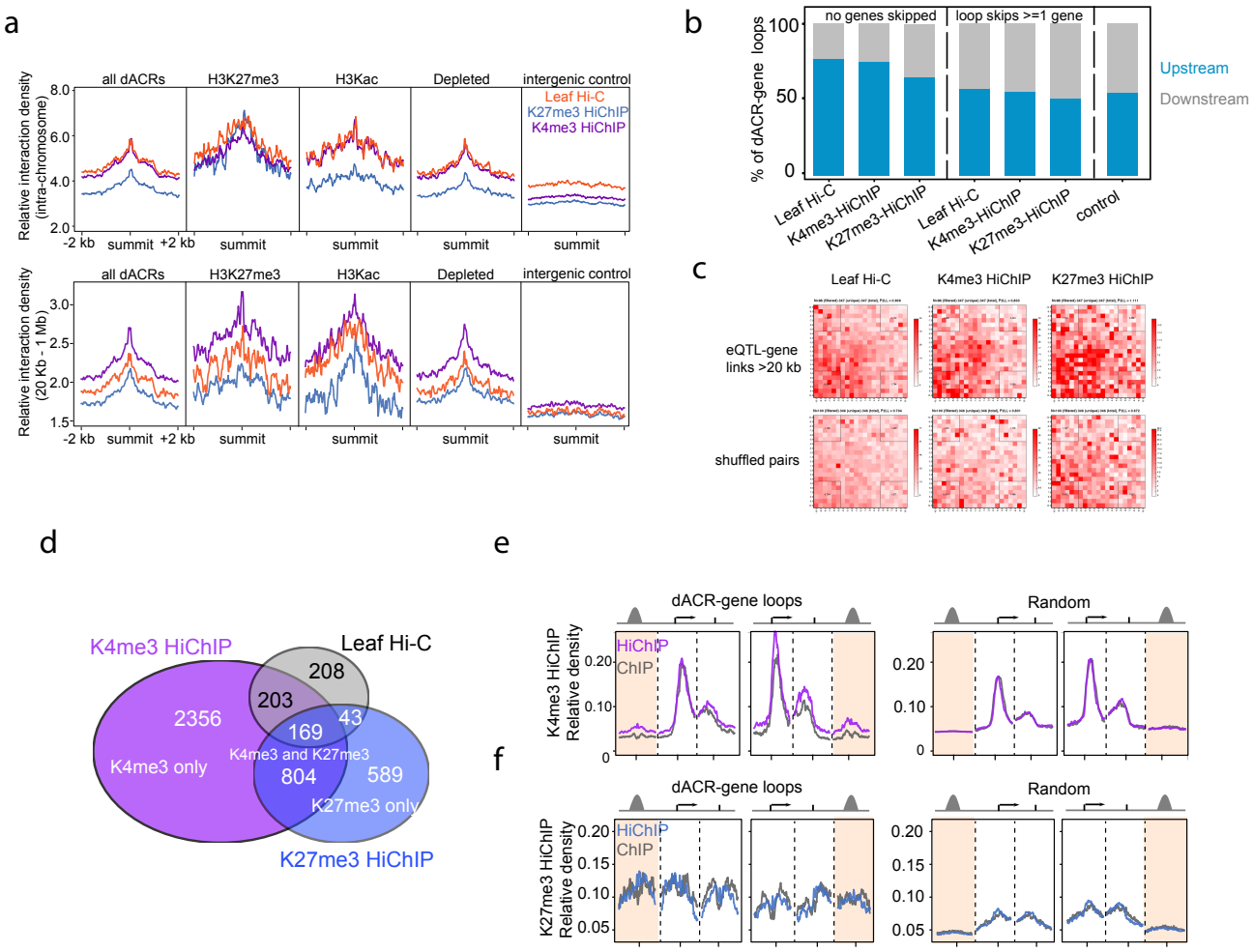

Supplementary Fig. 7 | Hi-C and HiChIP interactions at dACRs. a, Virtual 4C intrachromosomal interaction signals at dACR summits. Top panels show all intrachromosomal interactions and bottom panels show only interactions between 20 kb and 1 Mb. **b,** The percentages of dACR-gene loops in which the dACR resides either upstream or downstream of the target gene's promoter. dACR-gene pairs were split into those crossing over other genes and those not crossing any other genes. Sample sizes (left to right): 837, 5357, 4051, 449, 5876, 4218, 1000. **c,** Aggregate Peak Analysis (APA) showing the Hi-C/HiChIP interaction signals at the eQTL-gene pairs, compared to randomly permuted, genomic-distance-constrained dACRs and genes. The eQTL-gene pairs show enhanced Hi-C/HiChIP interactions. **d,** The overlap of dACR-gene loops from Hi-C, K4me3 HiChIP and K27me3 HiChIP. **e,** H3K4me3 ChIP signal was enriched at the TSS of expressed genes, but absent from the dACRs that were looped with the genes. **f,** H3K27me3 ChIP signal was enriched at the both the dACR and TSS of dACR-gene K27me3 HiChIP loops. Hi-C and HiChIP experiments were performed as single biological replicates.

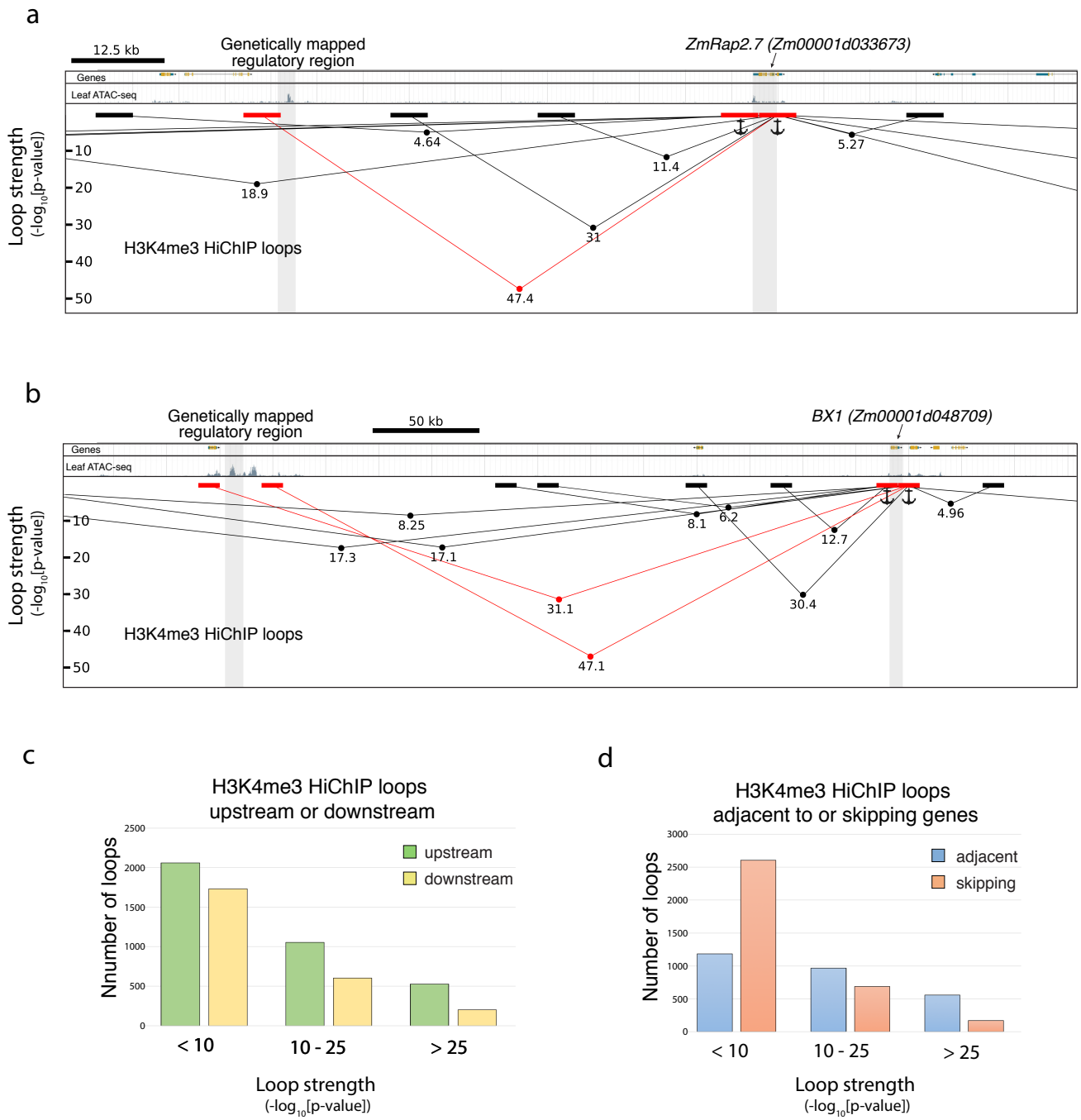

Supplementary Fig. 8 | Loop strength at agronomic QTL and loop numbers for various orientations relative to target genes. a, Browser shot of the *ZmRAP2.7* locus and its genetically fine-mapped predicted CRE. **b**, Browser shot of the *BX1* locus and its genetically fine-mapped predicted CRE. **c**, Number of H3K4me3 HiChIP loops with dACRs positioned upstream of target genes' promoters versus downstream, separated by loop statistical significance. **d**, Number of dACR-gene H3K4me3 HiChIP loops which link adjacent dACRs and genes, versus linking dACRs and genes that are separated by one or more genes in between (skipping). All p-values shown in figures were determined in the FitHiChIP program utilizing a two-tailed binomial test.

Data Table S5. Summary statistics of MethylC-seq

No	Sample	Length (nt)	Total reads	Aligned reads*	Non-conversion (%)	Genome coverage
1	B73 leaf	125*2	636,294,670	310,612,031	0.36%	36.38

* Uniquely aligned non-clonal reads

Data Table S6. Summary statistics of RNA-seq

No	Sample	Length (nt)	Total reads	Uniquely aligned	%	Multiple aligned	%
1	B73 leaf rep1	75	46,421,549	37,629,479	81.1%	5,849,616	12.6%
2	B73 leaf rep2	75	45,672,397	35,856,199	78.5%	5,663,861	12.4%
3	B73 inflorescence rep1	150	55,742,012	46,845,242	84.0%	5,640,111	10.1%
4	B73 inflorescence rep2	150	74,438,862	62,322,494	83.7%	7,667,537	10.3%
5	B73 inflorescence rep3	150	72,358,047	57,554,374	79.5%	7,001,809	9.7%
6	B73 inflorescence rep4	150	58,987,597	47,535,124	80.6%	5,639,592	9.6%

Data Table S7. Summary statistics of ATAC-seq, STARR-seq and ChIP-seq

Data type	Sample	Length (nt)	Total reads	Aligned reads	%
ATAC-seq	B73 leaf rep1	35*2	95,964,379	77,472,312	80.73%
ATAC-seq	B73 leaf rep2	35*2	571,321,741	451,685,647	79.06%
ATAC-seq	B73 inflorescence rep1	35*2	76,811,222	56,582,127	73.66%
ATAC-seq	B73 inflorescence rep2	35*2	174,903,747	87,212,919	49.86%
STARR-seq	B73 DNA input	35*2	41,763,217	35,679,215	85.43%
STARR-seq	B73 RNA	35*2	69,363,243	55,613,533	80.18%
ChIP-seq	B73 leaf H2AZ rep1	75	27,732,267	26,486,801	95.51%
ChIP-seq	B73 leaf H2AZ rep2	75	19,252,409	18,399,538	95.57%
ChIP-seq	B73 leaf H3K4me1 rep1	75	48,198,327	46,208,231	95.87%
ChIP-seq	B73 leaf H3K4me1 rep2	75	48,459,950	46,294,226	95.53%
ChIP-seq	B73 leaf H3K4me3 rep1	75	14,706,000	13,658,703	92.88%
ChIP-seq	B73 leaf H3K4me3 rep2	75	14,206,461	11,497,814	80.93%
ChIP-seq	B73 leaf H3K9ac rep1	75	23,017,373	22,278,839	96.79%
ChIP-seq	B73 leaf H3K9ac rep2	75	42,990,103	41,542,119	96.63%
ChIP-seq	B73 leaf H3K27ac rep1	75	50,627,599	49,003,001	96.79%
ChIP-seq	B73 leaf H3K27ac rep2	75	51,044,191	49,430,997	96.84%
ChIP-seq	B73 leaf H3K27me3 rep1	75	24,095,651	23,474,756	97.42%
ChIP-seq	B73 leaf H3K27me3 rep2	75	24,046,522	23,478,832	97.64%
ChIP-seq	B73 leaf H3K36me3 rep1	75	49,208,879	47,247,742	96.01%
ChIP-seq	B73 leaf H3K36me3 rep2	75	75,396,238	72,412,977	96.04%
ChIP-seq	B73 leaf H3K56ac rep1	75	14,631,000	13,604,127	92.98%
ChIP-seq	B73 leaf H3K56ac rep2	75	30,604,762	29,571,854	96.63%
ChIP-seq	B73 leaf H3 rep1	75	46,542,831	43,533,860	93.54%
ChIP-seq	B73 leaf H3 rep2	75	15,137,000	14,418,690	95.25%
ChIP-seq	B73 leaf input rep1	75	22,716,315	21,335,884	93.92%
ChIP-seq	B73 leaf input rep2	75	20,824,166	19,559,465	93.93%
ChIP-seq	B73 inflorescence H3K4me3 rep1	75	42,571,199	41,517,523	97.52%
ChIP-seq	B73 inflorescence H3K4me3 rep2	75	44,288,396	42,644,295	96.29%
ChIP-seq	B73 inflorescence H3K27me3 rep1	75	78,963,021	75,414,392	95.51%
ChIP-seq	B73 inflorescence H3K27me3 rep2	75	72,768,893	70,398,382	96.74%
ChIP-seq	B73 inflorescence H3K36me3 rep1	75	41,183,792	40,282,556	97.81%
ChIP-seq	B73 inflorescence H3K36me3 rep2	75	56,234,785	54,357,330	96.66%
ChIP-seq	B73 inflorescence H3K56ac rep1	75	20,524,329	19,544,866	95.23%
ChIP-seq	B73 inflorescence H3K56ac rep2	75	38,591,965	37,530,383	97.25%
ChIP-seq	B73 inflorescence H3 rep1	75	13,843,701	13,474,764	97.33%
ChIP-seq	B73 inflorescence input rep1	75	33,165,873	32,379,611	97.63%

Data Table S8. Summary statistics of Hi-C

	B73 leaf rep1	B73 leaf rep2	B73 leaf rep3	B73 leaf rep4	B73 leaf rep5	B73 leaf rep6	B73 leaf merged	Paired reads (%)
Total_pairs_processed	91,218,236	112,000,000	118,000,000	173,000,000	106,000,000	94,261,611	694,479,847	/
Unmapped_pairs	491,771	1,900,777	4,645,751	6,207,808	6,691,319	5,078,380	25,015,806	3.60%
Low_qual_pairs (multi-mapping)	62,042,480	76,337,699	79,263,318	118,000,000	67,622,383	61,371,165	464,637,045	66.90%
Unique_paired_alignments	25,618,714	29,800,633	28,106,664	40,094,016	25,855,705	22,968,300	172,444,032	24.83%
Multiple_pairs_alignments	0	0	0	0	0	0	0	/
Pairs_with_singleton	3,065,271	3,838,670	6,021,255	8,932,041	5,574,669	4,843,766	32,275,672	/
Low_qual_singleton	0	0	0	0	0	0	0	/
Unique_singleton_alignments	0	0	0	0	0	0	0	/
Multiple_singleton_alignments	0	0	0	0	0	0	0	/
Reported_pairs	25,618,714	29,800,633	28,106,664	40,094,016	25,855,705	22,968,300	172,444,032	24.83%
Valid_interaction_pairs	22,037,183	23,372,211	21,046,197	30,062,199	16,966,690	15,706,013	129,190,493	18.60%
Valid_interaction_pairs_FF	5,485,723	5,815,606	5,249,394	7,497,467	4,221,396	3,911,314	32,180,900	/
Valid_interaction_pairs_RR	5,481,926	5,817,225	5,241,079	7,493,350	4,220,781	3,908,401	32,162,762	/
Valid_interaction_pairs_RF	5,456,262	5,782,669	5,209,937	7,441,862	4,197,800	3,893,111	31,981,641	/
Valid_interaction_pairs_FR	5,613,272	5,956,711	5,345,787	7,629,520	4,326,713	3,993,187	32,865,190	/
Dangling_end_pairs	3,437,915	6,209,275	6,809,185	9,673,006	8,606,742	7,024,555	41,760,678	6.01%
Religation_pairs	114,893	128,287	101,862	132,755	104,326	82,793	664,916	0.10%
Self_Cycle_pairs	28,302	90,282	148,646	225,167	177,199	154,441	824,037	0.12%
Single-end_pairs	0	0	0	0	0	0	0	0.00%
Dumped_pairs	421	578	774	889	748	498	3,908	0.00%
valid_interaction	22,037,183	23,372,211	21,046,197	30,062,199	16,966,690	15,706,013	129,190,493	18.60%
valid_interaction_rmdup	21,469,859	22,706,721	19,911,029	28,006,068	16,503,930	15,274,208	123,871,815	17.84%
trans_interaction	9,035,156	9,646,159	6,236,837	9,411,588	5,297,148	5,191,594	44,818,482	6.45%
cis_interaction	12,434,703	13,060,562	13,674,192	18,594,480	11,206,782	10,082,614	79,053,333	11.38%
cis_shortRange (<20k)	1,976,020	2,129,440	2,138,604	2,881,181	1,649,003	1,424,887	12,199,135	1.76%
cis_longRange (>20k)	10,458,683	10,931,122	11,535,588	15,713,299	9,557,779	8,657,727	66,854,198	9.63%

Data Table S9. Summary statistics of HiChIP

	H3K4me3	Paired reads (%)	H3K27me3	Paired reads (%)
Total_pairs_processed	326,790,696	/	373,824,484	/
Unmapped_pairs	6,891,622	2.11%	7,327,488	1.96%
Low_qual_pairs (multi-mapping)	203,735,261	62.34%	246,489,441	65.94%
Unique_paired_alignments	104,559,206	32.00%	107,187,533	28.67%
Multiple_pairs_alignments	0	/	0	/
Pairs_with_singleton	11,604,607	/	12,820,022	/
Low_qual_singleton	0	/	0	/
Unique_singleton_alignments	0	/	0	/
Multiple_singleton_alignments	0	/	0	/
Reported_pairs	104,559,206	32.00%	107,187,533	28.67%
Valid_interaction_pairs	85,952,971	26.30%	89,774,346	24.02%
Valid_interaction_pairs_FF	21,376,712	/	22,309,423	/
Valid_interaction_pairs_RR	21,374,430	/	22,295,825	/
Valid_interaction_pairs_RF	21,081,403	/	22,037,893	/
Valid_interaction_pairs_FR	22,120,426	/	23,131,205	/
Dangling_end_pairs	16,067,350	4.92%	15,042,473	4.02%
Religation_pairs	686,585	0.21%	747,142	0.20%
Self_Cycle_pairs	1,849,735	0.57%	1,620,087	0.43%
Single-end_pairs	0	0.00%	0	0.00%
Dumped_pairs	2,565	0.00%	3,485	0.00%
valid_interaction	85,952,971	26.30%	89,774,346	24.02%
valid_interaction_rmdup	71,724,261	21.95%	52,485,887	14.04%
trans_interaction	19,351,764	5.92%	13,984,287	3.74%
cis_interaction	52,372,497	16.03%	38,501,600	10.30%
cis_shortRange (<20k)	13,515,142	4.14%	9,972,259	2.67%
cis_longRange (>20k)	38,857,355	11.89%	28,529,341	7.63%

Data Table S10. Summary statistics of DAP-seq

No	Sample	Length (nt)	Total read*	Aligned reads	%	MAPQ > 30	%
1	BAD1	75	5,417,421	5,385,760	99.42%	2,925,671	54.32%
2	BZIP25	75	13,642,865	13,582,792	99.56%	7,363,265	54.21%
3	BZIP54	75	13,196,410	13,139,452	99.57%	7,206,373	54.85%
4	BZIP57_FEA4	75	25,985,097	25,818,283	99.36%	13,864,652	53.70%
5	BZIP72	75	10,895,725	10,852,766	99.61%	5,894,672	54.31%
6	BZIP96	75	10,330,472	10,273,254	99.45%	5,551,721	54.04%
7	EREB127	75	4,357,850	4,316,436	99.05%	2,378,062	55.09%
8	EREB138	75	10,362,804	10,288,525	99.28%	6,421,780	62.42%
9	EREB24_BBM	75	28,297,699	28,129,669	99.41%	14,489,873	51.51%
10	EREB29	75	8,757,185	8,698,027	99.32%	5,334,257	61.33%
11	EREB71-rep1	75	11,787,059	11,676,857	99.07%	6,280,947	53.79%
12	LBD16_RA2	75	27,975,475	27,779,002	99.30%	15,681,385	56.45%
13	LBD19_IG1	75	16,700,403	16,589,953	99.34%	10,886,229	65.62%
14	LBD38	75	14,255,281	14,177,747	99.46%	7,684,190	54.20%
15	LBD5	75	16,642,239	16,541,913	99.40%	8,937,884	54.03%
16	SBP30_UB3	75	10,169,207	10,091,075	99.23%	5,924,112	58.71%
17	SBP6	75	10,682,140	10,603,571	99.26%	6,052,893	57.08%
18	SBP8_UB2	75	10,690,459	10,608,533	99.23%	6,298,605	59.37%

***** After quality trimming with trimmomatic

Data Table S11. Antibodies used for ChIP and HiChIP

epitope	source	cat #	used in
H2A.Z	in-house		ChIP
H3	Abcam	Cat# ab1791	ChIP
H3K4me1	Abcam	Cat# ab8895	ChIP
H3K4me3	Millipore	Cat# 07-473	ChIP, HiChIP
H3K9me2	Cell Signaling	Cat# 9753L	ChIP
H3K9ac	Active Motif	Cat# 61251	ChIP
H3K23ac	Millipore	Cat# 07-355	ChIP
H3K27me3	Millipore	Cat# 07-449	ChIP, HiChIP
H3K27ac	Abcam	Cat# ab4729	ChIP
H3K36me3	Abcam	Cat# ab9050	ChIP
H3K56ac	Millipore	Cat# 07-677-1	ChIP
RNA polII	Abcam	Cat# ab26721	ChIP

Data Table S12. Coordinates of regions omitted from STARR-seq analyses

2:19452127..19589055
8:135887933..136051059
4:3582270..3781476
1:270433990..270585643
8:67224311..67419905
6:120633193..120880806

Table s12. The STARR-seq sequencing data showed some cross-contamination with six bacterial artificial chromosomes derived from the B73 v4.0 reference genome. The six regions listed contained the contamination and were omitted from STARR-seq analyses.